JOURNAL OF CATALYSIS **130**, 29–40 (1991)

Iron Oxide Pillared Clay with Large Gallery Height: Synthesis and Properties as a Fischer–Tropsch Catalyst

EDWARD G. RIGHTOR, MING-SHIN TZOU, AND THOMAS J. PINNAVAIA[1]

Department of Chemistry and Center for Fundamental Materials Research, Michigan State University, East Lansing, Michigan 48824

Received August 22, 1990; revised January 17, 1991

New iron oxide pillared montmorillonites have been prepared by the reaction of Na^+ montmorillonite with base-hydrolyzed solutions of Fe^{3+} salts and subsequent thermal conversion of the intercalated polycations. Depending on the hydrolysis conditions used to generate the pillaring solutions, pillared products with basal spacings in the range 18 to 25 Å were obtained. Under optimum hydrolysis conditions (base/metal = 2.0 meq/mol, aging time = 23–147 hr) the pillared products contained 6.8–9.8 Fe^{3+} ions per $O_{20}(OH)_4$ unit cell and exhibited basal spacings of 25–29 Å. These latter spacings corresponded to exceptionally large gallery heights of 15–19 Å. Upon calcination at 300°C, the spacings decreased to 23–27 Å. N_2 BET surface areas after outgassing at 350°C were in the range 270 to 350 m^2/g. The pillared products are active catalysts that have undergone Fischer–Tropsch synthesis of hydrocarbons at 275°C and 120 -psi ($CO : H_2 = 1 : 2$). The hydrocarbon distribution in the C_1–C_6 range (1.3% conversion) followed Anderson–Schulz–Flory statistics with a chain propagation probability of $\alpha = 0.49$. X-ray energy dispersive analysis indicated that substantial amounts of the intercalated iron migrated to the edge sites of the clay particles under reaction conditions. The redistribution of iron resulted in a distribution of gallery heights sufficiently heterogeneous to preclude Bragg X-ray scattering along the 001 direction. Iron migration also occurred upon exposure of the pillared products to the ambient atmosphere for prolonged periods ($\geq$3 months).

INTRODUCTION

Pillared clays were first introduced by Barrer and Macleod in 1955 when they induced permanent porosity in smectite clays by propping open the clay layer with intercalated tetraalkylammonium ions (*1*). Various robust organic cations and metal chelates have been successfully used to pillar smectites, but these systems tend to undergo interlayer collapse above 300°C (*2*). Pillaring reagents formed by the hydrolysis of chromium (*3*), aluminum (*3–7*), bismuth (*8*), silicon (*9, 10*), and zirconium (*11*) afford intercalated oxide aggregates that are considerably more robust than organic pillars. Thermal stabilities exceeding 500°C have been reported (*6, 12*) for aluminum and zirconium oxide pillared clays. These thermally stable systems continue to be of interest, in part, because of their properties as catalysts for hydrocarbon cracking (*13–16*), alcohol dehydration (*17–19*), and other acid-promoted reactions (*20, 21*).

The aqueous chemistry of Fe^{3+} is known to yield polymeric cations (*22, 23*) of substantial size, and there have been reported attempts to intercalate such ions in the interlayers of smectite clays (*24–30*). Polymerization of iron typically begins at low pH (<1.5) and propagates by deprotonation of coordinated water molecules (olation) and hydroxygroups (oxolation) as illustrated in Eqs. (1) and (2) (*31*).

$$[Fe(OH)_2^+]_n + Fe^{3+} + 2H_2O \rightarrow [Fe(OH)_2^+]_{n+1} + 2H^+ \quad (1)$$

$$[Fe(OH)_2^+]_n \rightarrow [FeO(OH)]_n + H_n^+ \quad (2)$$

The hydrolysis reactions of Fe^{3+} can lead to discrete spherical polycations as large as

---

[1] To whom correspondence should be addressed.

0021-9517/91 $3.00

30 Å in diameter (*32, 33*). Aggregation of the spheres produces rods and eventually rafts of rods. The polymerization process is dependent on base to metal ratio, temperature, nature of the counterion, pH, and other factors (*31, 34*).

Earlier attempts to intercalate Fe^{3+} polymeric cations in smectities yielded products with relatively low gallery heights and limited thermal stabilities (approximately 300°C) (*24–29*). In the present study, we have examined the intercalated products formed by the reaction of sodium montmorillonite with base-hydrolyzed Fe^{3+} solutions under different hydrolysis conditions. These studies have led us to new iron oxide pillared clays with basal spacings up to 28 Å, a value substantially larger than the 16.7 Å materials derived from utilized basic trinuclear iron(III) acetate as the pillar precursor (*35*). Since iron oxide is known for its activity as a Fischer–Tropsch catalyst (*36–38*), we also have examined one of these new pillared products for the catalytic hydrogenation of carbon monoxide.

EXPERIMENTAL SECTION

Pillaring Reactions

Anhydrous sodium carbonate was added slowly as a powder to a rapidly stirred solution of 0.2 *M* iron(III) nitrate, chloride, or perchlorate. The amount of base added was in the range 0.0 to 2.5 meq/mole of metal. The solutions, which were free of a precipitate, were flushed with nitrogen to facilitate the removal of the carbon dioxide that was evolved during the hydrolysis. The solutions were then aged for various periods of time at specified temperatures to allow for different degrees of polycation growth. The general procedures used for the exchange reaction between the hydrolyzed iron solutions and sodium montmorillonite (Crook County, Wyoming) were similar to those previously described for the synthesis of aluminum pillared montmorillonite (*39*). A 1.0 wt.% suspension of the clay was added slowly to a vigorously stirred solution of the iron polycations. The ratio of cation to clay was 70 mmol/meq for most syntheses. The material used for the catalytic Fischer–Tropsch reactions was prepared at a cation to clay ratio of 30 mmol/meq. Upon the complete addition of clay to the hydrolyzed Fe^{3+} solution, the reaction mixture was stirred for an additional 2 hr. The product was then washed to remove excess salt by the process of subsequent centrifugation, decantation, addition of deionized water, and redispersal of the product by vigorous stirring in water. The product typically was washed 12 or more times or until flocculation of the clay occurred upon washing. The resulting material was then air-dried on a glass plate at room temperature.

Physical Methods

A Phillips X-ray diffractometer (Ni-filtered Cu$K\alpha$) was used to determine the basal spacings of the pillared products. Samples for XRD measurements were prepared by allowing a 1 wt% slurry from the final washing to air dry on a glass slide. Diffraction patterns also were recorded after heating the slide for 3 hr in air at 350°C. Elemental analyses were performed on a Jarrel–Ash 995 Atom Comp analyzer. Instra-grade standards (J. Baker) were used to calibrate the instrument, and the results were checked against a NIST standard clay (98a). Catalyst samples (0.05 g) for chemical analyses were fused with lithium borate for 2.0 min at 1000°C and the resulting hot glass was dissolved in 3% HNO_3.

Surface area measurements based on the three-point BET method were determined on a Perkin–Elmer–Shell 212 sorptometer using nitrogen as the adsorbate and helium as a carrier gas. The gases were purified by passing through a liquid nitrogen trap. Prior to analysis, samples were outgassed at 350°C under a flow of argon for 2 hr.

Catalysis

Fischer–Tropsch reactions were carried out in a 304 stainless steel, single-pass tube reactor. Gas flow rates were controlled by a Brooks 5890 mass flow controller. Approximately 0.3 g of pillared clay was mixed with enough low surface area γ-alumina (10–14 mesh) to make a bed height of 7 cm in a reactor tube with a 7 mm inside diameter. A thermocouple clad in 304 stainless steel was placed in the middle of the bed for temperature regulation by a Eurotherm temperature controller.

The catalyst was dried in helium at 400°C at a gas hourly space velocity (GHSV) of 300 hr^{-1} and then cooled to 25°C. The gas flow as then changed to hydrogen (GHSV $= 428\ h^{-1}$) and reduction of the catalyst was carried out by ramping the temperature to 200°C for 30 min and then to 400°C for 16 hr. The reactor was cooled to room temperature, and the flow was switched to a premixed feed gas ($H_2/CO = 2.0$) at a GHSV of 300 hr^{-1}. The temperature was then increased to 275°C and the pressure was increased to 120 psi. Condensible liquids were trapped in an elbow attached to the reactor tube. The elbow was cooled in a dry ice–acetone bath. Hydrocarbon fractions were sampled through a sampling valve using a valved, gas-tight syringe and analyzed on an F & M scientific gas chromatograph by flame ionization. A Porapak Q column was used to separate permanent gases for analysis on a Varian 920 gas chromatograph. Alkane and alkene standards (Scott Specialty Gases) were used for calibration. Permanent gases (CO_2, CO) were separated using a Carbosieve S-11 column and TCD detection.

Electron Microscopy

Air-dried iron pillared clay samples for scanning electron microscopy (SEM) were wedged between two pieces of wood applicator sticks. A conductive liquid was applied around the base and exterior of the catalyst particles and atop the wood segments to minimize charging. A light coat of gold was then evaporated onto the samples using a sputter coater. SEM was performed with a JEOL JSM 35 C electron microscope equipped with a Kevex X-ray energy dispersive detector (EDS) and a Tracor Northern digital beam controller. EDS linescans were obtained by a computer-controlled point-by-point scan of the electron beam across the sample.

TABLE 1

Iron Pillared Clays Formed from Hydrolyzed Ferric Chloride and Nitrate Solutions[a]

B/M (meq/mol)	$FeCl_3$		$Fe(NO_3)_3$	
	Pillaring soln. pH	Clay basal spacing (Å)	Pillaring soln. pH	Clay basal spacing (Å)
0.0	1.38	12.3	1.25	12.3
0.5	1.40	19.8	1.52	18.0
1.0	1.53	23.8	1.65	23.2
1.5	1.60	24.5	1.75	23.2
2.0	1.72	25.2	1.82	23.8
2.5	2.18	[b]	2.05	[b]

[a] Reaction conditions: $[Fe^{3+}] = 0.2\ M$; Fe^{3+}/montmorillonite = 70 mmol/meq; temp. = 25°C; aging time of pillaring solution = 24 hr.

[b] Very broad 001 peak centered near 16 Å.

RESULTS AND DISCUSSION

Synthesis of Iron Oxide Pillared Clays

The iron oxide pillared clays formed by the reaction of sodium montmorillonite with hydrolyzed Fe^{3+} solutions depended critically on the hydrolysis conditions. Table 1 shows the relationship between the base to metal ratio (*B/M*) used for the hydrolysis of ferric chloride and nitrate solutions, along with the basal spacing of the products formed upon reaction with sodium montmorillonite. In each case the time allowed for aging of the pillaring reagent was held constant at 24 hr. Solutions with $B/M = 0.0$ gave products with a low basal spacing near 12.3 Å, corresponding to a gallery height of ~3.0 Å. Incremental increases in *B/M* ratio over the range 0.5 to 2.0 resulted in dramatic increases in basal spacing in the range 18 to 25 Å. The abrupt increase in spacing beginning at $B/M = 1.0$ points to the more or less uniform intercalation of a polymer fraction. The observed gallery heights are consistent

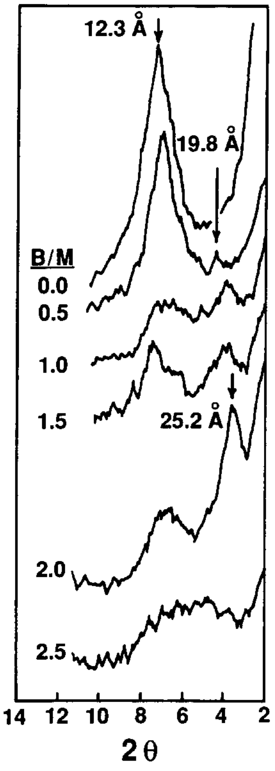

FIG. 1. X-ray diffraction patterns of air-dried iron pillared clays prepared from hydrolyzed ferric chloride solutions (0.2 *M*) at base to metal ratios in the range 0.0–2.5 meq/mol. Solid Na_2CO_3 was used as the base and the aging time of the pillaring solutions was 24 hr in each case.

with the previously estimated size of 15 to 30 Å for polycations formed by iron hydrolysis in this *B*/*M* range (*32, 33*). The relatively small increase in basal spacing for the pillared products over the *B*/*M* range 1.0–2.0 was indicative of limited growth in the polymer along the 001 direction of the host clay.

Figure 1 illustrates the XRD patterns for the pillared products obtained from ferric chloride pillaring solutions with $B/M = 0.0 - 2.5$. Note that the low 2Θ peak was initially positioned near 19.8 Å and that the peak was relatively weak, indicating that the extent of ordered pillaring was relatively low at $B/M < 0.5$. As the *B*/*M* ratio was increased, the peak for the pillared product shifted to higher basal spacing and increased in intensity. At a $B/M = 2.0$, two orders of 001 reflection were observed, corresponding to a basal spacing of 25.2 Å (gallery height ~15.9 Å). However, at $B/M = 2.5$, the product was highly interstratified with a broad first-order reflection centered near 16 Å. Thus, the most ordered product was obtained at $B/M = 2.0$. The interstratification which occurred at $B/M = 2.5$ may be due to the presence of a distribution of polycation sizes. The latter possibility is supported by the previously reported (*32, 33*) bimodal sedimentation values for 0.10 *M* $FeCl_3$ solutions hydrolyzed at $B/M = 2.5$.

Hydrolyzed solutions of the nitrate salt of Fe^{3+} exhibited pillaring properties analogous to those observed for the chloride salt, as judged from the basal spacings of the pillared products (cf. Table 1). Similar spacings also were found for the products formed from hydrolyzed solutions of ferric perchlorate. Previous studies (*23, 31–34*) of Fe^{3+} hydrolysis have shown that the extent of iron aggregation can be anion dependent. For instance, the polymerization of hydrolyzed chloride solutions is bimodal (*31*), whereas nitrate solutions exhibit unimodal behavior. Despite these differences in aggregation for the chloride and nitrate salts, hydrolysis of both salts under appropriate conditions gave pillared products with similar basal spacings. However, a dramatic anion effect was found for solutions formed by hydrolysis of Fe^{3+} in the presence of sulfate. Sulfate readily complexes with iron and promotes precipitation of hydrolyzed products (*31*). Thus, ferric sulfate always afforded non-pillared products with basal spacings of ~12.6 Å, regardless of the *B*/*M* ratio used in the hydrolysis.

All of the products described in Table 1 and Fig. 1 were extensively washed with deionized water prior to being air-dried. The washing process is extremely important for producing crystalline pillared products. At least twelve was cycles were normally needed before the flocculation of the product was observed. The relationship between the product crystallinity, flocculation, and

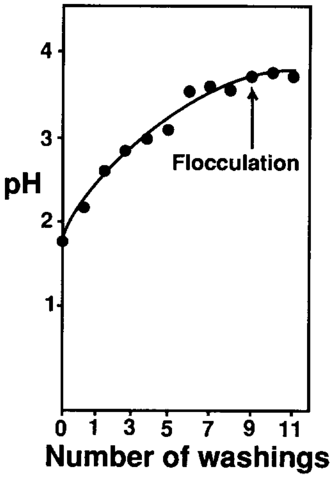

FIG. 2. pH of wash solution vs number of washings for a pillared clay prepared by reaction of Na$^+$-montmorillonite with a hydrolyzed ferric chloride solution (B/M = 2.0 meq/mol; 24-hr aging time). The arrow indicates the point at which the clay suspension flocculated and where a distinct 001 X-ray reflection was evident at 25.2 Å.

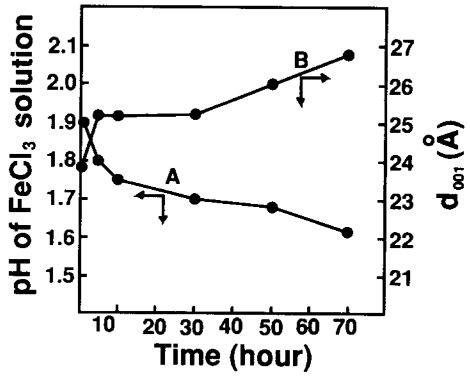

FIG. 3. (A) Dependence of pillaring solution pH on ageing time for a ferric chloride solution hydrolyzed at 25°C and B/M = 2.0. (B) Dependence of the basal spacings of pillared products on the aging time of the pillaring solution.

degree of washing suggested that hydrolysis of the clay-bound polycations continued during the wash cycle. For pillaring solutions with $B/M \geq 1.0$, the products tended to be amorphous, if they were not washed to the flocculation point. Apparently, the initial products formed were highly interstratified and the irregular basal spacings gave rise to little or no Bragg scattering along 001. However, as washing was continued, hydrolysis becomes more extensive, the polycation size became more uniform, and the gallery heights became sufficiently regular to exhibit Bragg scattering.

Support for the hydrolysis of the surface-bound iron cations during the wash cycle was provided by the data shown in Fig. 2, where the pH of the wash solution is plotted vs the number of washings for a product formed by the reaction of Na$^+$-montmorillonite with a pillaring solution prepared at B/M = 2.0. The pH continued to rise with the number of washings until a limiting value of approximately 3.9 was approached after the 11th wash and flocculation of the clay had occurred. Significantly, no Bragg X-ray scattering was apparent until the sample had been washed at least 9 times.

We should note at this point that our synthesis methods have recently been utilized (*40*) in an effort to produce iron pillared clays for the demetallation of crude oil and the absorption of H_2S (*41, 42*). However, the products obtained were highly interstratified, X-ray amorphous phases with high surface area. The formation of amorphous phases most likely was the result of inadequate washing and insufficient hydrolysis of the intercalated polycations.

The aging time of the hydrolyzed pillaring solutions also was important in determining the nature of the pillared products. Figure 3 illustrates the change in pH for a 0.2 M ferric chloride solution hydrolyzed at 25°C by the addition of sodium carbonate at B/M = 2.0. As expected for an increase in the degree of cation polymerization, the pH of the solution decreased with aging time up to 70 hr. Shown in the same figure is the relationship between the basal spacing of the pillared product and the aging time of the pillaring solution. An overall increase of approximately 2 Å was observed upon extending the aging time from 10 to 70 hr. The relatively small increase in basal spacing despite

TABLE 2

Compositions of Iron Pillared Clays[a]

Pillaring soln.			Pillar/cell[b]	S.A. m_2/g[c]	d_{001}(Å)	
Salt	Age (hr)	pH			25°C	350°C
$FeCl_3$	24	1.72	$[Fe(OH)_{2.94}^{0.06+}]_{9.75}$	244	25.2	22.8
$Fe(NO_3)_3$	3	1.92	$[Fe(OH)_{3.92}^{0.08+}]_{6.83}$	351	27.2	24.5
	147	1.73	$[Fe(OH)_{3.93}^{0.07+}]_{8.80}$	270	29.5	27.6
$Fe(ClO_4)_3$	3	1.89	$[Fe(OH)_{2.90}^{0.10+}]_{6.12}$	343	26.8	24.5

[a] All products were prepared from pillaring solutions formed by hydrolysis of Fe^{3+} salt solutions (0.2 *M*) at 25°C using a base to metal ratio $B/M = 2.0$ meq/mol and solid Na_2CO_3 as the base.

[b] Iron content of pillared products expressed as hydroxyiron (III) per $O_{20}(OH)_4$ unit.

[c] BET N_2 surface area after outgassing 3 hr at 350°C in vacuum.

the appreciable drop in pH and extent of hydrolysis was suggestive of uniaxial polymer growth. Anisotropic polymer growth would be consistent with the results of Murphy *et al.* (*33b*) who observed the formation of short rods from spherical polycations after 24 hr of aging at $B/M = 2.0$. The rod diameters were estimated to be 20 Å, and the rod lengths were 60 to 100 Å.

Further evidence for polycation rod or rafts in the clay galleries was provided by the analytical data and BET surface areas provided in Table 2. Limiting the hydrolysis of iron at a $B/M = 2.0$ by restricting the aging time to 3 hr at 25°C produced products containing 6.1 to 6.8 Fe^{3+} ions per $O_{20}(OH)_4$ unit cell. Increasing the extent of polymerization by increasing the aging time to 24 hr of 7 days, produced pillar products containing 8.8 to 9.8 iron ions per unit cell. The average charge per iron was in the range 0.06–0.10, based on the assumption that the clay layer charge is unaltered by pillaring. In providing the pillar formulas in the table, we arbitrarily selected hydroxide as the counterion to express the average iron charge. The actual polycation, however, is expected to contain both oxide and hydroxide counterions (*30, 31*).

A change in iron composition was accompanied by a change in the BET surface areas from approximately 345 m^2/g for the products containing 6.1–6.8 Fe/cell to between 244 and 270 m^2/g for the materials containing 8.8–8.9 Fe/cell. The decrease in surface area with increasing iron content, along with the absence of a dependence of basal spacing on composition, suggested that ion polymerization in the gallery was restricted to aggregates with rod-like or raft-like morphology.

We breifly explored the possibility that pillared products with basal spacings different from ~26 ± 2 Å might be accessible using pillaring solutions prepared by hydrolysis below and above ambient temperature. Accordingly, a 0.2 *M* $FeCl_3$ solution was hydrolyzed at 0°C and $B/M = 2.0$. After aging 24 hr at 0°C, the pillaring reagent was allowed to react with Na^+-montmorillonite both at 0 and at 25°C. Regardless of the reaction temperature or the temperature at which the pillared clay product was washed, the basal spacings were near the value obtained when the hydrolysis was carried out at 25°C.

Hydrolysis of 0.2 *M* $FeCl_3$ at 75°C and at $B/M = 2.0$ also afforded a pillared product with a basal spacing near 26 Å, provided that the aging time of the solutions was limited to 1.5 hr. Solutions aged >5 hr at 75°C were unsuitable as pillaring reagents owing to precipitate formation. Thus, varying the hydrolysis temperature of 0.2 *M* $FeCl_3$ over the range 0–75°C at $B/M = 2.0$ had little effect on the basal spacing of the pillared product formed by reaction with Na^+-montmorillonite.

Catalysis

The iron oxide pillared clays prepared in this work can be activated for Fischer–Tropsch catalysis by pretreating in hydrogen at 400°C for 16 hr. Previous studies have shown that the reaction of α-Fe_2O_3 with hydrogen at 350°C for 16 hr leads to the formation of metallic iron, as judged by X-ray diffraction and Mössbauer spectroscopy (*43*). Reduction of iron also is known to occur in the reaction of magnetite (Fe_3O_4) with hydrogen at 497°C (*44*). Earlier XPS and Mössbauer studies (*45*, *46*) of montmorillonite interlayered with iron polycations have established the presence of Fe(III) ions in octahedral environments. Although the gallery height of our pillared clay is larger than previously reported derivatives, we expect a similar reduction of Fe(III) to occur under the hydrogen pretreatment conditions used in the present work.

The distribution of C_1 to C_6 hydrocarbons formed in the hydrogenation of carbon monoxide followed the Anderson–Schulz–Flory relationship (*36*)

$$W_n = n\alpha^{n-1}[1 - \alpha]^2,$$

where W_n is the weight fraction of product with carbon number n and α is the probability of stepwise chain growth. Figure 4 provides the C_1–C_6 distribution obtained for Fischer–Tropsch synthesis at 275°C over a pillared montmorillonite containing 6.98 Fe^{32} ions per $O_{20}(OH)_4$ unit (d_{001} = 25.2 Å; 298 m^2/g). Under the reaction conditions employed (H_2/CO = 2.0, 120 psi, GHSV = 2100 hr^{-1}, 21 hr time-on-stream) the conversion was 1.3% and the chain propagation probability was 0.49. Increasing the conversion to 2.1% by decreasing the space velocity gave the same value of α within experimental uncertainty. Very small quantities of oxygenates, mainly methanol and ethanol in 2 : 1 ratio and a trace of propanol, were detectable in the aqueous phase trapped at −78°C.

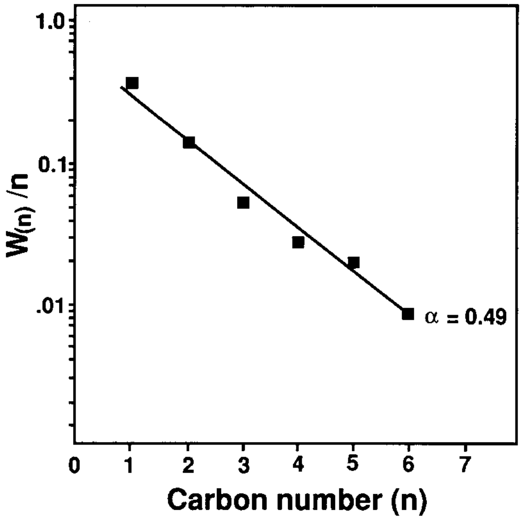

FIG. 4. The Anderson–Schulz–Flory plot of the hydrocarbon distribution obtained for the hydrogenation of CO over iron pillared montmorillonite after 21 hr on stream. Reaction conditions: 275°C, 120 psi, H_2/CO = 2.0, GHSV = 2100 hr^{-1}.

In general, the conversion initially increased with increasing time-on-stream and then decreased at longer reaction times (≥125 hr). Similar behavior has been observed for related iron-based Fischer–Tropsch catalysts (*43*, *47*). After a reaction time of 50 hr the catalyst contained 1.18 wt% carbon, suggesting the possible formation of coke. No attempt was made to extract and identify the adsorbed species.

In order to minimize product hold-up effects and, especially, the possibility of coke formation, relatively low conversions were utilized in determining α for our pillared clay catalyst. Although the conversions are low, the value of 0.49 at 275°C is similar to the propagation probabilities found for related iron-based catalysts under analogous reaction conditions. For instance, Accuri *et al.* (*44*) observed α = 0.43 at 2% conversion over a silica-supported prereduced iron catalyst under related reaction conditions (206 psi, 250°C, H_2/CO = 3.0). Using magnetite catalyst precursors prepared under different

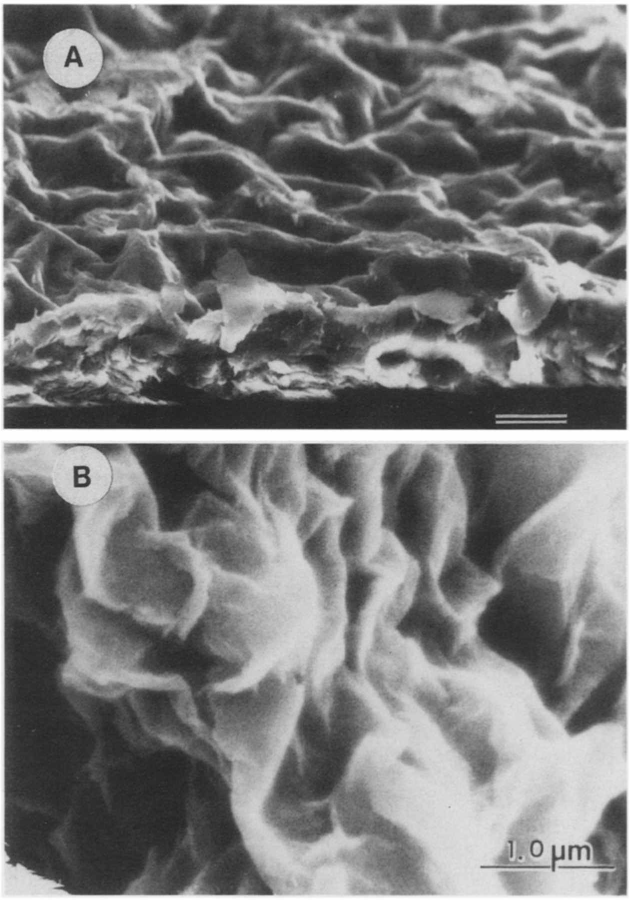

FIG. 5. SEM images illustrating the folded or "waffle-like" surface texture of Na^+-montmorillonite. The bar represents 10 μm in micrograph A, 1.0 μm in micrograph B.

prereduction conditions, Krebs *et al.* (*48*) observed α values in the range 0.39–0.46 for Fischer–Tropsch synthesis at 298°C ($H_2/CO = 3.0$; 1 bar). Also, Dictor and Bell (*47*) observed $\alpha = 0.53$ [C_1–C_8] for Fischer–Tropsch synthesis carried out at <5% conversion in a slurry reactor over hydrogen-reduced hematite at 250°C and 147 psi.

SEM and EDS Studies

Scanning electron microscopy and X-ray energy dispersive spectroscopy were utilized to investigate the texture and iron distribution of an iron oxide pillared clay before and after Fischer–Tropsch catalysis. The air-dried clay before catalysis exhibited a distinctly lamellar texture, as expected. Interestingly, however, the folded or "waffle-like" surface texture typical of air-dried Na^+-montmorillonite was substantially reduced upon pillaring by the iron polycations. The change in texture upon pillaring is illustrated by the SEM images in Figs. 5 and 6 for Na^+-montmorillonite and iron pillared montomorillonite, respectively. Although the iron pillared clay had a more platey texture than the Na^+ exchange form, and exhibited much more intense 001 X-ray diffraction peaks.

EDS linescans for iron and silicon in the native Na^+-montmorillonite indicated that

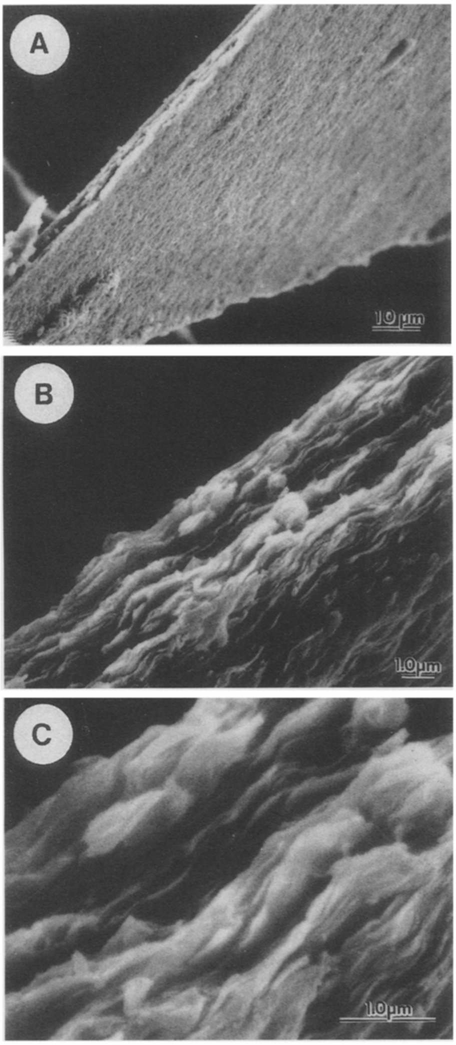

FIG. 6. SEM images of iron pillared montmorillonite with a smooth platey surface texture. The bar represents 10 μm in micrograph A and 1.0 μm in micrographs B and C.

the two elements were uniformly distributed. However, the Fe^{3+} X-ray emission intensity was just above background, whereas the Si X-ray intensity was high, as expected based on the relative abundance of the two elements. After pillaring by polycations of iron, the clay gave similar iron and silicon EDS linescans, except that the iron emission was much more intense, comparable to the emission intensity of silicon. Thus, the spatial distribution of the pillaring iron species was uniform on a micrometer length scale for the freshly prepared pillared products.

In order to examine the hydrolytic stability of the pillared clay under ambient conditions, the material was allowed to age in the open atmosphere. Substantial changes were observed in the iron distribution by EDS after aging 3 months, as shown in Fig. 7. Although the iron and silicon content paralleled each other across the basal surfaces, a dramatic increase in iron and a decrease in silicon occurred at the edge of the clay particle. An EDS examination of the edges of an iron-bearing Na^+-montmorillonite showed that the increase in emission intensity at the clay edge was far greater than would be expected due to edge-selective emission effects of a compositionally uniform particle. Thus, we conclude that exposing the iron pillared clay sample to the moist ambient atmosphere resulted in the migration of some iron ions out of the gallery and onto the edges of the clay particles. This change in iron distribution was accompanied by a loss in 001 X-ray reflections.

Calcining the iron pillared clay at 350°C in air did not improve its stability toward moist air. Hydrolytic instability and redistribution of iron also was apparent for the iron pillared clay after use as a Fischer–Tropsch catalyst for 24 hr under the reaction conditions described in Fig. 4. The spent catalyst also was X-ray amorphous. The production of water in the Fischer–Tropsch reaction most likely facilitated the migration of the gallery iron.

SUMMARY AND CONCLUSIONS

The hydrolysis of ferric chloride, nitrate, or perchlorate solutions at a base to metal ratio of 2.0 meq/mol afforded polycations of iron that were suitable for the pillaring of montmorillonite. The products obtained by the reaction of the polycations with Na^+-montmorillonite at Fe/clay = 30–70 mmol/meq were crystallographically poorly ordered along the 001 layer stacking direction,

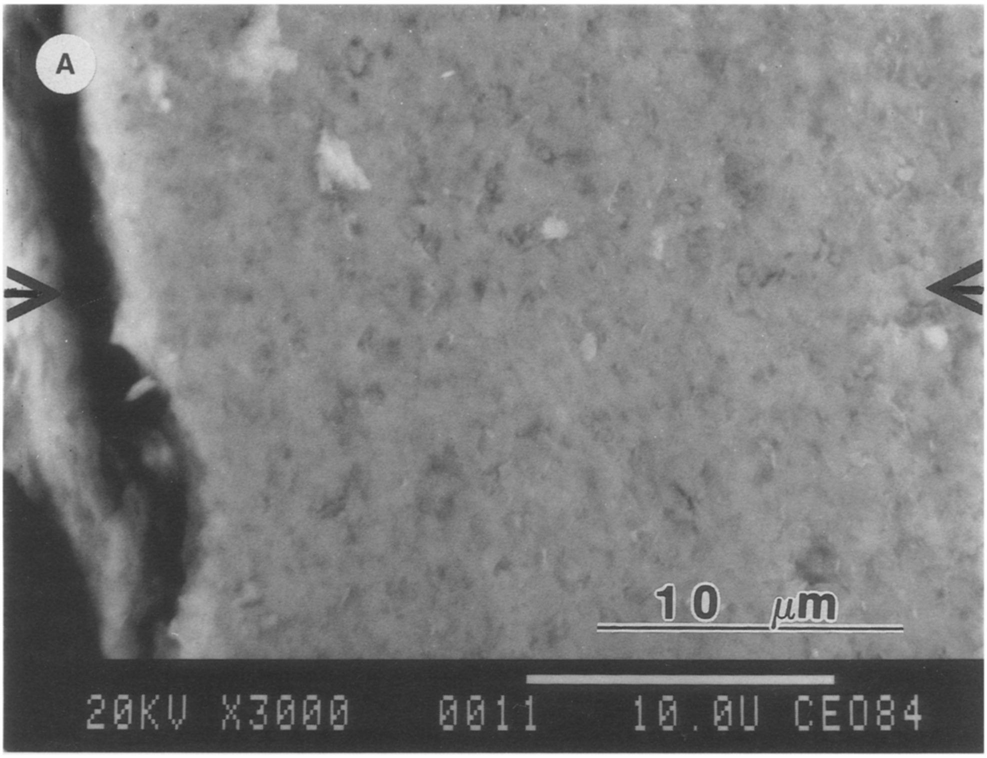

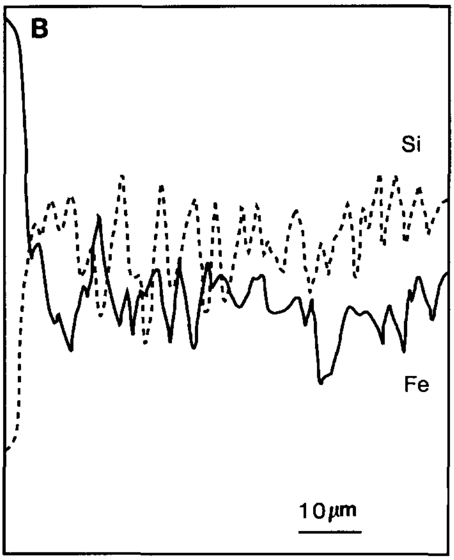

FIG. 7. (A) SEM and (B) Si and Fe X-ray EDS line scans for iron pillared montmorillonite after aging 3 months under ambient conditions. The arrows in the SEM image indicate the direction of the EDS line scan.

most likely due to a distribution of intercalated pillar sizes. The degree of 001 ordering was improved by extensively washing the product with distilled water. The washing process represented a second hydrolysis step in which ensembles of polymeric cations with rod- or raft-like structures were reconstituted on the clay basal surfaces into more regular oxocation aggregates that give rise to a basal spacing of 26 ± 2 Å. The basal spacings were substantially larger than those previously reported for pillared products obtained by hydrolysis of basic iron acetate cations ($d_{001} \sim 16.7$ Å) (*35*, *46*).

Products containing 6.1–9.8 Fe^{3+} ions per $O_{20}(OH)_4$ unit cell were obtained after aging the pillaring solutions 3–168 hr at room temperature. The decrease in surface area with increasing iron content over this composition range, along with the absence of a dependence of basal spacing on iron content, was consistent with a rod-like or raft-like pillar structure.

The iron pillared clays reported here were quite labile even under ambient conditions. Aging the materials for periods of 3 months at 25°C resulted in a loss of 001 ordering due to a redistribution of iron and a concomitant change in the degree of polycation polymerization. X-ray energy dispersive spectroscopy indicated that some iron migrated to particle edges upon aging. Calcining the materials at 350°C did not improve the stability toward iron redistribution.

Fischer–Tropsch synthesis of hydrocarbons was achieved over iron pillared clays. Prereduction in hydrogen at 400°C afforded an active catalyst for CO hydrogenation at 275°C, and 120 psi. The hydrocarbon distribution over the C_1–C_6 range followed the Anderson–Schulz–Flory model with a chain propagation probability of $\alpha = 0.49$ at 1.3 to 2.1% conversion. The value of α was not unlike that observed for iron oxide supported on alumina. Crystallographic ordering of the catalyst along with 001 layer stacking direction was lost during Fischer–Tropsch synthesis. The water formed as a reaction by-product most likely facilitated the reconstitution of polyoxoiron pillars.

ACKNOWLEDGMENTS

This research was supported in part by the National Science Foundation and by the MSU Center for Fundamental Materials Research.

REFERENCES

1. Barrer, R. M., and Macleod, D. M., *Trans. Faraday Soc.* **52,** 1290 (1955).
2. Loeppert, R. H., Mortland, M. M., and Pinnavaia, T. J., *Clays Clay Miner.* **27,** 201 (1979).
3. Brindley, G. W., and Yamanaka, S., *Am. Miner.* **54,** 630 (1979).
4. Vaughan, D. E. W., and Lussier, R. J., *Proc. Int. Conf. Zeolites 5th, 1980.*
5. Lahav, N., Shani, V., and Shabtai, J., *Clays Clay Miner.* **24,** 107 (1978).
6. Brindley, G. W. and Sempels, R. E., *Clays Clay Miner.* **12,** 229 (1977).
7. Occelli, M. L., and Tindwa, T. M., *Clays Clay Miner.* **31,** 119 (1979).
8. Yamanaka, S., Yamashita, G., and Hattori, M., *Clays Clay Miner.* **28,** 281 (1980).
9. Endo, T., Mortland, M. M., and Pinnavaia, T. J., *Clays Clay Miner.* **28,** 105 (1980).
10. Endo, T., Mortland, M. M., and Pinnavaia, T. J., **29,** 153 (1981).
11. Yamanaka, S., and Brindley, G. W., *Clays Clay Miner.* **27,** 119 (1979).
12. Yamanaka, S., and Brindley, G. W., *Clays Clay Miner.* **21,** 21 (1978).
13. Pinnavaia, T. J., *Science* **220,** 265 (1983).
14. Lussier, R. J., Magee, J. S., and Vaughan, D. E. W., *in* "Preprints, 7th Canadian Symposium on Catalysis, Edmonton, Alberta, Canada, October 1980.
15. Occelli, M. L., *Ind. Eng. Chem. Prod. Res. Dev.* **22,** 553 (1983).
16. Occelli, M. L., Landau, S. D., and Pinnavaia, T. J., *J. Catal.* **90,** 250 (1984).
17. Birch, R., and Warburton, C. I., *J. Catal.* **97,** 511 (1986).
18. Galaway, A. K., *J. Catal.* **19,** 330 (1970).
19. Occelli, M. L., Innes, R. A. Hwu, F. S. S., and Hightower, J. W., *Appl. Catal.* **14,** 69 (1985).
20. Morikawa, Y., Goto, T., and Ikawa, Moro-Oka, *Chem. Lett.*, 1667 (1982).
21. Occelli, M. L., Husu, J. T., and Glya, L. G., *J. Mol. Catal.* **33,** 371 (1985).
22. Spiro, T. G., Allerton, S. E., Renner, J., Terzis, A., Bils, R., and Saltman, P., *J. Am. Chem. Soc.* **88,** 2721 (1966).
23. Sylva, R. N., *Rev. Pure Appl. Chem.* **115,** 22 (1972).
24. Page, A. L., Whittig, L. D., *Soil Sci. Soc. Am. Proc.* **25,** 282 (1961).

25. Carstea, D. D., *Clays Clay Miner.* **16,** 231 (1968).
26. Rengasamy, P., and Oades, J. M., *Aust. J. Soil Res.* **15,** 221 (1977).
27. Rengasamy, P., and Oades, J. M. *Aust. J. Soil Res.* **15,** 235 (1977).
28. Herrera, R., and Peech, M., *Soil Sci. Soc. Am. Proc.* **34,** 740 (1970).
29. Yamanaka, S., Doi, T., Sako, S., and Hattori, M., *Mat. Res. Bull.* **19,** 161 (1984).
30. Oades, J. M., *Clays Clay Miner.* **32,** 49 (1984).
31. Flynn Jr., C. M., *Chem. Rev.* **84,** 31 (1984).
32. Murphy, P. J., Posner, A. M., and Quirk, J. P., *Aust. J. Soil Res.* **13,** 189 (1975).
33. Murphy, P. J., Posner, A. M., and Quirk, J. P., *J. Colloid Interface Sci.* (a) **52,** 229 (1975); (b) **56,** 270 (1976); (c) **56,** 284 (1976); (d) **56,** 298 (1976); (e) **56,** 312 (1976).
34. Baes Jr., C. F., and Mesmer, R. E., "The Hydrolysis of Cations," p. 489. Wiley, New York, 1976.
35. Yamanaka, S., and Hattori, M., *Catal. Today* **2,** 261 (1988).
36. Storch, H. H., Golumbic, N., and Anderson, R. B., "The Fischer–Tropsch and Related Syntheses." Wiley, New York, 1951.
37. Ponec, V., *in* "Catalysis" (G. C. Bond and G. Webb, Eds.), Vol. 5, Specialist Periodical Reports. Chemical Society, London, 1982.
38. Dry, M. E., *in* "Catalysis" (J. R. Anderson and M. Boudart, Eds.), p. 159, Specialist Periodical Reports. Springer-Verlag, Heidelberg, 1981.
39. Pinnavaia, T. J., Tzou, M. S., Landau, S. D., and Raythatha, R. H., *J. Mol. Catal.* **27,** 3942 (1984).
40. Warburton, C. I. *Catal. Today* **2,** 271 (1988).
41. Burch, R., and Warburton, C. I., *Appl. Catal.* **33,** 395 (1987).
42. Burch, R., and Warburton, C. I., *J. Chem. Soc. Chem. Commun.* **2,** 117 (1987).
43. Niemantsverdriet, J. W., van der Kraan, A. M., van der Dijk, W. L., and van der Baan, H. S., *J. Phys. Chem.* **84,** 3363 (1980).
44. Accuri, K. B., Schwartz, L. H., and Piotrowski, and Butt, J. B., *J. Catal.* **95,** 349 (1984).
45. Doff, D. H., Gangas, N. H. J., Allan, J. E. M., and Coey, J. M. D., *Clay Miner.* **23,** 367 (1988).
46. Martin-Luengo, M., Martins-Carvalho, H., Ladriere, J., and Grange, P., *Clay Miner.* **24,** 495, (1989).
47. Dictor, R. A., and Bell, A. T., *J. Catal.* **97,** 121 (1986).
48. Krebs, H. J., Bonzel, H. P., Schwaring, W., and Gafner, G. *J. Catal.* **72,** 199 (1981).